EXPERIMENTAL

Vanessa Zambelli
Giuseppe Di Grigoli
Margherita Scanziani
Silvia Valtorta
Maria Amigoni
Sara Belloli
Cristina Messa
Antonio Pesenti
Ferruccio Fazio
Giacomo Bellani
Rosa Maria Moresco

Time course of metabolic activity and cellular infiltration in a murine model of acid-induced lung injury

V. Zambelli and G. Di Grigoli equally
contributed to this article.

V. Zambelli · M. Scanziani ·
M. Amigoni · A. Pesenti · G. Bellani (✉)
Department of Experimental Medicine
(DIMS), University of Milan-Bicocca,
Via Cadore 48, 20900 Monza, MB, Italy
e-mail: giacomo.bellani1@unimib.it
Tel.: +39-03-92333293
Fax: +39-03-92332297

V. Zambelli
Department of Cardiovascular Research,
Istituto di Ricerche Farmacologiche Mario
Negri, Milan, MI, Italy

G. Di Grigoli · S. Valtorta ·
C. Messa · F. Fazio · R. M. Moresco
Tecnomed Foundation, Foundation
of University of Milano-Bicocca,
Milan, MI, Italy

G. Di Grigoli · S. Valtorta ·
S. Belloli · C. Messa · R. M. Moresco
IBFM, CNR, Milan, Italy

M. Scanziani · M. Amigoni ·
A. Pesenti · G. Bellani
Department of Perioperative Medicine
and Intensive Care, San Gerardo Hospital,
Monza, MB, Italy

G. Di Grigoli · S. Valtorta · S. Belloli ·
C. Messa · F. Fazio · R. M. Moresco
Nuclear Medicine Department and PET
Centre, San Raffaele Scientific Institute,
Milan, MI, Italy

Abstract *Purpose:* This study
investigates whether positron emis-
sion tomography (PET) can be used
to monitor the inflammatory response
and its correlation with the later
fibroproliferative phase in an
experimental model of acute lung
injury. *Methods:* Hydrochloric acid
(0.1 N, pH 1, 1.5 ml/kg) was instilled
into the right bronchus of mice. A
group of mice underwent a micro-
computed tomography (CT) scan 1 h
after lung injury and a series of
2-[^{18}F]fluorine-2-deoxy-D-glucose
(FDG)-PET scans (6, 24 and 48 h and
7 days after surgery). After 21 days
respiratory static compliance was
assessed and lung tissue was collected
in order to measure the hydroxy

(OH)-proline content. Other groups of
mice underwent micro-CT and micro-
PET scans at the same time points,
and then were immediately killed to
assess arterial blood gases and his-
tology. *Results:* Histological
analysis showed the recruitment of
neutrophils and macrophages into the
damaged lung, reaching the peak at
24 and 48 h, respectively. The time
course of the [^{18}F]FDG signal, used
as a marker of inflammation, corre-
lated with that of recruited
inflammatory cells. In mice killed
21 days after the surgery, a correla-
tion was found between reduced
respiratory static compliance and high
PET signal 7 days after lung injury.
The PET signal also correlated with
the OH-proline content. *Conclu-
sions:* This study demonstrated that
PET imaging is a valid means of
tracking the inflammatory response,
also in longitudinal studies. More-
over, a correlation was found between
persistence of the inflammatory
response and fibrotic evolution of the
injury.

Keywords ALI · PET · [^{18}F]FDG ·
Neutrophils · Macrophages

Introduction

Acute lung injury (ALI) and acute respiratory distress syndrome (ARDS) are life-threatening forms of acute respiratory failure [1] with a high mortality rate ($\sim 40\%$) [2, 3]. The early phase is marked by arterial hypoxemia, alveolar capillary leakage and leukocyte extravasation. This phase may progress to a fibroproliferative process characterized by decreased lungs compliance [4]. We recently developed a murine model of regional acid aspiration that allows long-term animal survival: despite a recovery of gas exchange, we observed a persistent derangement in respiratory system compliance, associated with a fibrotic scar and inflammatory infiltrate [5].

The pathogenesis of ALI/ARDS is characterized by intrapulmonary and systemic inflammatory responses [6–8]. The inflammatory reaction is partially controlled by alveolar macrophages [9], which can initiate and modulate the recruitment of neutrophils (polymorphonu- clear cells, PMNs) in the lungs, where these cells can cause or contribute to parenchymal injury [10]. Chronic and poorly regulated inflammation can often lead to fibrosis [9], and macrophages are also considered important in this progression [11]. Despite improvements in ventilation strategies, there is still a need for effective pharmacological approaches, able to improve patient prognosis and to pre- vent the development of lung fibrosis.

Reduction of lung inflammation during the acute phase could be a target of pharmacological therapy. Recent studies [12–16] evaluated the effect of different drugs, but they used invasive procedures like post-mortem histology and regional evaluation of lung inflammation through analysis of bronchoalveolar lavage (BAL) fluid.

As already suggested [17], a tool like positron emis- sion tomography (PET), enabling the in vivo monitoring of inflammation, could help to increase the understanding of its role in the progression of ALI/ARDS; it could also allow the preclinical assessment of novel therapeutic strategies through a methodological approach that can be translated to the clinical research setting. The use of PET with 2-[^{18}F]fluorine-2-deoxy-D-glucose (FDG) has been applied to the estimation of lung inflammation in patients with ALI/ARDS [18–20] and, at the preclinical level, in different models of ALI/ARDS, including ventilator- induced lung injury (VILI) [21] and VILI plus endotox- emia [22]. Preclinical [23–27] and clinical studies [28, 29] have suggested that PMNs are, at least in the acute phase of injury, the dominant cell type. Nonetheless, other cells, such as endothelial ones, play a role in the metabolism- dependent radioactivity distribution [24, 30].

The primary objectives of this study were: (1) to evaluate whether [^{18}F]FDG-PET could be a useful tool for the in vivo monitoring of the inflammatory response in our previously described model of ALI [5] and (2) to establish whether [^{18}F]FDG uptake can provide an early marker of fibrotic evolution.

Materials and methods

Animals and induction of injury

Female CD-1 mice (22-28 g, Charles River Laboratories, Lecco, Italy) were used. All the procedures involving the animals and their care were conducted in conformity with the relative institutional guidelines which comply with relevant national (no. 116, G.U., suppl. 40, 18/2/1992, no. 8, G.U., 14/7/1994) and international laws and policies (EEC Council Directive 86/609, OJ L 358,1, Dec 12, 1987; Guide for the Care and Use of Laboratory Animals, US National Research Council, 1996). The acid-induced lung injury was performed as previously described [5]. Briefly, anesthetized animals were intubated and venti- lated with a tidal volume of 8–10 ml/kg, respiratory rate 130 min^{-1}, positive end-expiratory pressure 2 cm H_2O and FiO_2 1. The right bronchus was instilled with hydrochloric acid (HCl) (1.5 ml/kg of 0.1 N, pH 1). Mice were ventilated for 10 min, then extubated and placed in an oxygenated chamber (FiO_2 0.5) until full awakening.

Experimental design

The study was divided into two sets of experiments (see Electronic Supplementary Material, ESM, Fig. E1):

Longitudinal experiment

The same group of animals ($n = 9$–10) underwent a micro-computed tomography (CT) scan (1 h after acid instillation) and a series of [^{18}F]FDG-PET scans (6, 24 and 48 h and 7 days after surgery). At 21 days, these mice were killed and the lungs sampled for hydroxypro- line assay.

Single-point experiment

This part of the study was aimed at correlating imaging and histological findings. After induction of injury, five mice underwent CT and [^{18}F]FDG-PET scans at the same time points reported for the longitudinal study (1 h and 6, 24, 48 h and 7 days), after which they were killed and processed for histological analysis. We also evaluated the effect on left lung activity measurement of the spillover from the heart (see ESM).

A group of healthy (control) mice ($n = 11$) underwent a single [^{18}F]FDG-PET scan to evaluate [^{18}F]FDG lung uptake values in normal conditions (baseline levels).

Imaging procedures

CT imaging and analysis

Anesthetized mice (Tribromoethanol, Avertin® 2.5%, 400 mg/kg, ip) were placed prone on the CT table for lung scanning. CT scans were acquired using a MicroCT scanner (eXplore Locus, GE Healthcare) with the following parameters: 80 kV, 450 µA and 93-µm resolution. Images were analyzed using MicroView 2.1 software (GE Healthcare, see ESM).

PET imaging

PET imaging was performed using a YAP-(S)-PET II small animal scanner (ISE, Pisa, Italy) (field of view: 4×4 cm; maximum sensitivity: 19 cps/kBq; spatial resolution: 1.8 mm). Animals were fasted overnight before PET studies. The [^{18}F]FDG (4.2 ± 0.09 MBq in 50 µl of saline) was administered in the tail vein (see ESM). Mice were scanned for 30 min (6 frames of 5 min each) starting 45 min after [^{18}F]FDG administration. For each mouse, we obtained a mean [^{18}F]FDG uptake value, expressed as percentage of injected dose per gram of tissue (%ID/g). This was done by drawing circular regions of interest (ROIs) in the dorsal area of both lungs. These values were calculated by dividing the mean PET-measured values of calibrated radioactivity concentration in tissue (MBq/cc) by the injected doses (MBq) and multiplying by 100. In the longitudinal study, lung uptake data obtained 7 days after injury were expressed as the ratio between the right and left lung for the correlation with systemic static compliance (C_{stat}).

Assessment of injury

Longitudinal experiment

The assessment was performed 21 days after induction of injury:

Assessment of pressure-volume (PV) curves. Respiratory system PV curves were constructed in euthanized mice (sodium pentobarbital, 200 mg/kg, ip) immediately (within 5 min) after death in order to minimize postmortem muscle changes (see ESM).

Hydroxyproline assay. To estimate the development of fibrosis, the collagen content of lungs was measured using a conventional hydroxyproline method (see ESM) [31].

Single-point experiment

Animals were assessed at the previously specified time points, immediately after the micro-PET.

Arterial blood gas analysis. Anesthetized mice (Tribromoethanol, Avertin® 2.5%, 400 mg/kg, ip) were reintubated and mechanically ventilated as described above, and arterial blood gas analysis was performed (i-STAT, Burke & Burke S.p.A.).

Histological preparation and immunohistochemical staining. After exsanguination, the lungs were excised, weighed, fixed in 4% formalin for 24 h (at a pressure of 20 cmH$_2$O for the first 30 min), and then paraffin-embedded and sectioned. Staining for leukocyte-specific esterase and for macrophages was performed on 5 µm-thick paraffin-embedded sections (see ESM).

Statistical analysis

Data are expressed as mean $\pm$ SD. Variables at each time point were compared between the left and right lungs by paired t tests. Correlations between variables were tested by linear regression. P values of less than 0.05 were considered statistically significant. Fisher's r-to-z transformation was performed to establish the significance of the difference between two correlation coefficients. Statistical analyses were performed using GraphPad PRISM 5.03 (GraphPad software Inc., San Diego, CA) and by Sigmaplot 11.0 (Systat software Inc., Chicago, IL).

Results

Longitudinal experiment

Regions of low aeration, involving $61 \pm 19\%$ of the right lung, were observed in all animals on CT scans performed immediately after acid instillation.

No significant difference in [^{18}F]FDG uptake between the right and left lungs was found in the control group, evaluated in fasting condition (Table 1).

In the right lung of the HCl-treated animals, [^{18}F]FDG uptake (Table 1) was significantly higher than:

- [^{18}F]FDG uptake in the left lung at 6, 24 and 48 h, but not at 7 days post-injury;
- [^{18}F]FDG uptake in the right lung of fed and fasting control mice at all time points.

Uptake of [^{18}F]FDG was significantly higher in the left lung of HCl-treated mice than in the left lung of control mice studied in fasting condition.

Alterations in mechanical properties (C_{stat} 1.37 ± 0.09 ml*cmH2O-1*kg^{-1}) were observed 21 days after

Table 1 Time course of [^{18}F]FDG uptake (expressed as % ID/g) in longitudinal and single-point experiments at each time point in the right and left lungs

Time point	Longitudinal experiment		Single-point experiment	
	Right lung (n)	Left lung (n)	Right lung (n)	Left lung (n)
6 h	2.9 ± 0.4*,§,° (10)	2.3 ± 0.3**,# (10)	2.6 ± 0.3*,§,° (4)	1.6 ± 0.3** (4)
24 h	2.6 ± 0.4*,§,° (10)	1.9 ± 0.3** (10)	3.5 ± 0.5*,§,° (7)	2.2 ± 0.4** (7)
48 h	2.5 ± 0.6*,§,° (10)	2.0 ± 0.4** (10)	2.9 ± 0.8*,§,° (4)	1.5 ± 0.1** (4)
7 days	2.2 ± 0.4§,° (10)	2.0 ± 0.3** (10)	1.9 ± 0.2§ (4)	1.7 ± 0.1** (4)
	Right lung (n = 11)		Left lung (n = 11)	
Baseline (fasting)	1.4 ± 0.3		1.3 ± 0.2	
Feeding condition	1.63 ± 0.4		1.85 ± 0.4	

* $p < 0.05$ compared with contralateral lung
§ $p < 0.05$ compared with fasting group right lung
° $p < 0.05$ compared with feeding group right lung

** $p < 0.05$ compared with fasting group left lung
# $p < 0.05$ compared with feeding group left lung

lung injury. Interestingly, at 21 days, C_{stat} was closely correlated (R^2 0.73, $p = 0.003$) with [^{18}F]FDG levels (expressed as right/left ratio) measured 7 days after injury (Fig. 1). Moreover the hydroxyproline content in the right lung was closely correlated (R^2 0.55, $p = 0.01$) with the PET signal at 7 days after lung injury (Fig. 2), while no correlation was found for the left side. No correlations were found between the PET signal at the other time points (6, 24 and 48 h) and either C_{stat} or hydroxyproline content after 3 weeks (p = n.s. for all comparisons, data not shown).

Single-point experiment

Pulmonary function

As expected [5], monolateral HCl instillation induced a deterioration in gas exchange at 6 and 24 h (PaO$_2$ was 54 ± 6 and 67 ± 3 mmHg, respectively). At 48 h oxygenation recovered, remaining above 100 mmHg thereafter.

Time course of inflammatory cell accumulation in lung tissue

[^{18}F]FDG uptake (Fig. 3) in the right lung was significantly higher than in the contralateral lung up to 48 h after injury. As in the longitudinal study, uptake values returned to baseline values 7 days after HCl administration (Table 1). The [^{18}F]FDG uptake values for both lungs of the injured animals were statistically different at each time point compared to the values recorded in control group mice. Correction for lung tissue density did not modify the shape of [^{18}F]FDG uptake (see ESM, Fig. E6),
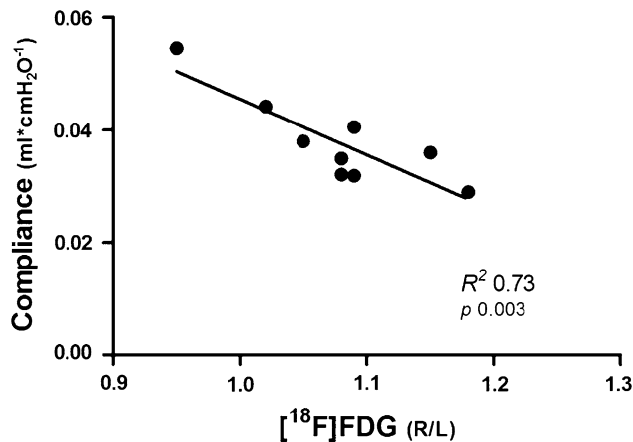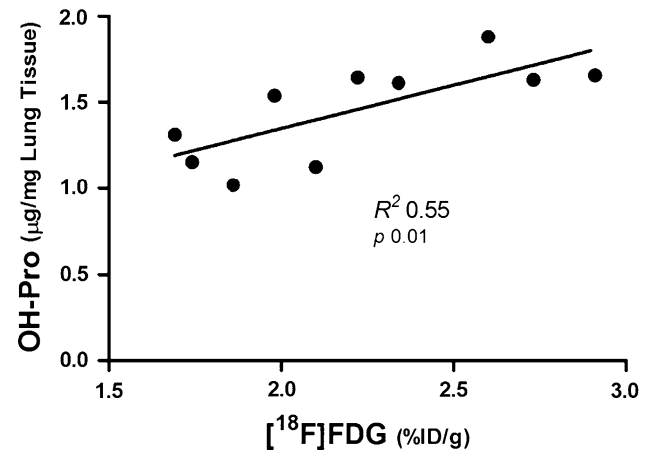

Fig. 1 Longitudinal experiment: relationship between [^{18}F]FDG uptake [expressed as right/left (R/L) ratio] at 7 days post-lung injury and respiratory system static compliance after 21 days ($n = 9$)

Fig. 2 Longitudinal experiment: relationship between [^{18}F]FDG uptake (expressed as % ID/g) at 7 days post-lung injury and OH-proline content after 21 days in the right lung ($n = 10$)

Fig. 3 Control group transaxial images divided into feeding and fasting condition and examples of HCl group images at 6 and 24 h after acid instillation. In CT images of HCl animals, the dashed *circles* represent the positions of *ROIs* in one of the lung slices used for the analysis
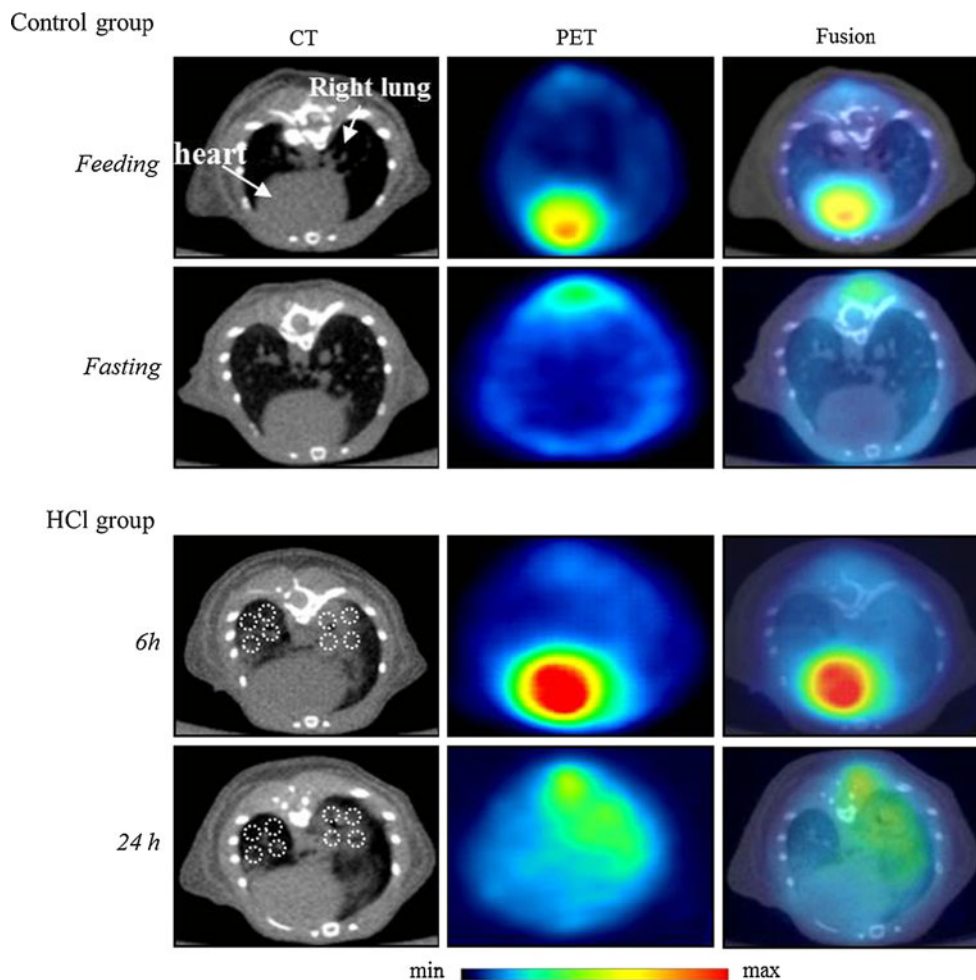
although it did reduce the difference between the right and left lungs (see ESM).

Inflammatory cell accumulation

PMN counts differed between the right and left lungs at 24, 48 h and 7 days (24 h: 172 ± 44 vs. 86 ± 11; 48 h: 50 ± 6 vs. 35 ± 4; 7 days: 27 ± 5 vs. 12 ± 3 per HPF; $p < 0.05$ for all comparisons), while macrophage counts differed at 6, 48 h and 7 days (6 h: 83 ± 8 vs. 59 ± 10; 48 h: 137 ± 10 vs. 66 ± 3; 7 days: 81 ± 8 vs. 54 ± 9 per HPF; $p < 0.05$ for all comparisons). In both lungs, the time course of the [18F]FDG uptake mirrored (see ESM, Fig. E3) that of the recruitment of PMNs and macrophages, peaking at around 24 h when PNMs were prevalent. Later, the concentration of PMNs decreased, and the [18F]FDG uptake mainly reflected the presence of macrophages. The PMN count correlated with [18F]FDG uptake both in the right (R^2 0.302, $p = 0.018$) and left lung (R^2 0.365, $p = 0.008$). Conversely, the number of macrophages did not correlate with PET [18F]FDG uptake (right lung R^2 0.033; left lung R^2 0.09). However, the correlation coefficients increased (albeit not significantly) if the sum of the two cell types was taken into account both in the right (R^2 0.41, $p = 0.01$) and in the left (R^2 0.50, $p = 0.003$) lung (Fig. 4).

MicroCT scan analysis

CT analysis 6 h after injury revealed an increased percentage of hypoaerated tissue in both lungs, [5]. Conversely, at 24 and 48 h, areas of abnormal density were differently ($p < 0.001$) distributed between the right and the left lung, being partially resolved at 7 and 21 days (see ESM, Fig. E4). [18F]FDG uptake correlated with the amount of hypoaerated tissue in the right lung (R^2 0.24, $p = 0.03$) but not in the left one (see ESM, Fig. E5).

Fig. 4 Single-point experiment: correlation between [18F]FDG uptake (expressed as %ID/g) and the number of PMNs and macrophages on tissue sections (expressed as n/HPF) at 6, 24, 48 h and at 7 days post-injury ($n = 18$) in the right (**a**) ($p = 0.01$) and left (**b**) ($p = 0.003$) lungs
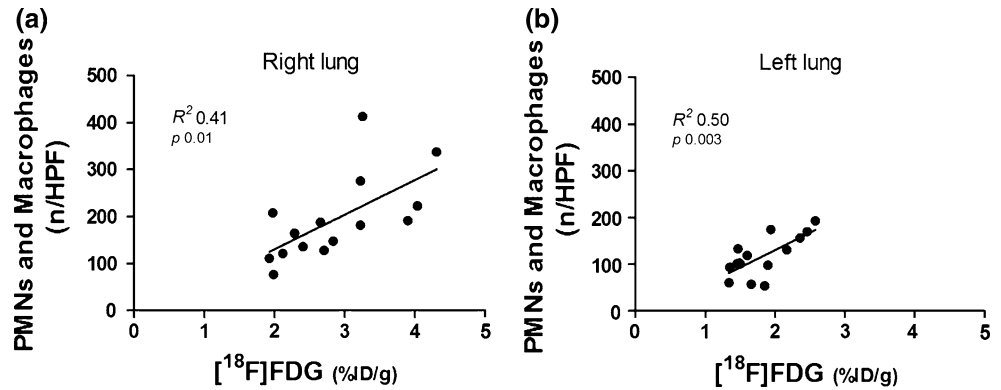
Discussion

The main purpose of this study was to characterize a method for the in vivo PET monitoring of lung inflammation in a previously developed model of ALI [5], and to explore the potential relationship between the acute inflammatory process and the late fibrotic evolution of the injury. Although it has been reported that the incidence of ALI is decreasing [32], its mortality rate is not, and at present no etiological therapies exist. The availability of a reliable and non-invasive technique for assessing the anti-inflammatory effect of different interventions might enhance the development of novel therapeutic strategies. In our model of unilateral acid aspiration lung injury [5], we showed recruitment of neutrophils and macrophages into the lung, beginning 6 h after injury and peaking at 24 and at 48 h, respectively. After 7 days the number of neutrophils decreased almost to baseline, whereas the macrophage count remained raised. Our data on neutrophil kinetics are in line with results reported by Reutershan et al. [33]. Interestingly, we found a significant correlation between [18F]FDG uptake (used as an in vivo marker of inflammation in this study) and the number of inflammatory cells recruited into the lung at all the considered time points after injury. The correlation was higher when the sum of PMNs and macrophages was taken into account as opposed to the single cell types. We considered that both types of cells are recruited during inflammation and may contribute to the [18F]FDG signal. However, as shown in Fig. E3 (ESM), their respective levels change over time. Whereas the observed time course of the [18F]FDG signal seemed to be more influenced by neutrophils in the first 48 h, 7 days after it probably depended more on the activity of the macrophages. Even though previous in vitro cell studies have demonstrated that monocytes and macrophages cannot increase their glucose uptake to the same extent as neutrophils can [34, 35], other authors, in in vivo (PET) and ex vivo (autoradiography) studies, have demonstrated that FDG is taken up by macrophages (particularly if activated) in different inflammatory diseases and malignancies [36–38]. Our results after 24 and 48 h are consistent with previous findings by Jones et al. [27] demonstrating, in a different model of lung inflammation, that [18F]FDG-PET may be used as an in vivo index of neutrophil recruitment. With regard to the later phase, we found that PET signal persisted in the lungs 7 days after injury, even though markedly reduced in comparison with the [18F]FDG uptake at 24 h. Other studies [26] demonstrated that persistence of the [18F]FDG uptake is associated with scarring of lung tissue. Similarly, in our study, the PET signal measured at 7 days showed a correlation with C_{stat} and with collagen deposition (as hydroxyproline content) measured at 21 days post-injury. Although it is not known whether post-mortem muscle changes affected the measurements of C_{stat}, we sought to minimize this possible bias by performing this measurement early after euthanasia. These data support the hypothesis that persistent inflammation in the lungs could lead to a fibrotic evolution of the injury.

In addition, analysis of the micro-CT scan results revealed a significant correlation between the percentage of hypoaerated tissue and the inflammatory signal measured by PET; this could be due to variability in the extent of the experimentally induced injury or to differences in the inflammatory response to the injury, leading to different amounts of edema and cellular infiltrate. However, the percentage of hypoaerated tissue did not correlate with the subsequent fibrotic evolution, suggesting that the increased amount of fibrosis was not solely due to a greater amount of injury.

Human data on the time course of lung metabolic activity during ALI are lacking. The fact that the increase in [18F]FDG uptake observed in the present study also spread to the left lung, found to be normally aerated on CT scan, is in line with human data showing increased [18F]FDG uptake in normally aerated areas [19]. However, these results should be interpreted cautiously because of the radioactivity spillover effect from myocardial [18F]FDG uptake. This effect could lead, in fact, to an overestimation of the radioactivity in the areas surrounding the heart, including the left lung. However, 6 h after injury, when most of the animals displayed myocardial uptake, the left lungs had reached levels

significantly higher than those observed in the feeding condition, indicating the presence of measurable levels of lung inflammation also in the left lung, as further supported by the significant correlation between cellular infiltration and [^{18}F]FDG uptake. In accordance with previous lung inflammation models, we observed an increased [^{18}F]FDG uptake in the myocardium particularly evident at 6 h and 7 days after HCl instillation (see ESM). Pawlik et al. [39] showed that hypoxic vasoconstriction caused acute pulmonary hypertension and increased right systolic pressure. Under these stressors, myocardial cells shift their metabolism from fatty acid to glucose oxidation. However, further studies are needed to clarify the molecular and functional bases of this shift.

Our study presents some limitations. First, we did not ascertain the cell type responsible for the PET signal, performing microautoradiography with tritiated deoxyglucose ([^{3}H]-DG) [23, 26, 27] or with [^{18}F]FDG [38, 40], nor did we used 11C-(R)-PK11195 for selective imaging of macrophages [41]. However, it is known [42] that, in some conditions, macrophages may be phenotypically different as regards the expression of the binding site of PK11195. Furthermore, PET data were not analyzed using a full quantitative method (e.g., Patlak's plot). On the other hand, this simple and non-invasive method does not require vessel cannulation. In addition, we did not perform PET scans at 21 days and therefore cannot exclude that further information might have been obtained at this later time point, even though at 7 days the PET signal was already very low. In addition, although we evaluated regional [^{18}F]FDG activity, we did not correct for tissue density in order to avoid overnormalization of data, since several reasons could account for the increased tissue density, including edema. The issue of regional distribution of inflammatory cell-dependent [^{18}F]FDG signal in normally aerated and affected lung might be explored in further studies using immunohistochemistry. In comparison with other available techniques, such as BAL or histology, the use of micro-PET to assess the intensity of inflammation has a limited sensitivity, but it offers two main advantages: first, the lack of invasiveness allows the application in longitudinal studies performed in the same experimental subject; second, the imaging procedure could be translated to the clinical research setting.

In conclusion, preclinical FDG-PET imaging allowed, non-invasively, a periodic monitoring of the inflammatory response in an experimental model of ALI/ARDS. Our findings show that the persistence of the [^{18}F]FDG signal after the acute phase is associated with an alteration of the lung compliance measured 2 weeks later, possibly attributable to the fibrotic evolution of injury promoted by the inflammatory infiltrate. Thus, it is possible, in our opinion, that acute treatments of the inflammation capable of reducing the fibroproliferative process could be monitored using the FDG-PET method.

References

1. Steinberg KP, Hudson LD (2000) Acute lung injury and acute respiratory distress syndrome. The clinical syndrome. Clin Chest Med 21:401–417
2. Rubenfeld GD, Caldwell E, Peabody E, Weaver J, Martin DP, Neff M, Stern EJ, Hudson LD (2005) Incidence and outcomes of acute lung injury. N Engl J Med 353:1685–1693
3. Ware LB, Matthay MA (2000) The acute respiratory distress syndrome. N Engl J Med 342:1334–1349
4. Bachofen M, Weibel ER (1982) Structural alterations of lung parenchyma in the adult respiratory distress syndrome. Clin Chest Med 3:35–56
5. Amigoni M, Bellani G, Scanziani M, Masson S, Bertoli E, Radaelli E, Patroniti N, Di Lelio A, Pesenti A, Latini R (2008) Lung injury and recovery in a murine model of unilateral acid aspiration. Anesthesiology 108:1037–1046
6. Abraham E (2003) Neutrophils and acute lung injury. Crit Care Med 31(Suppl 4):S195–S199
7. Wittkowski H, Sturrock A, van Zoelen MA et al (2007) Neutrophil-derived S100A12 in acute lung injury and respiratory distress syndrome. Crit Care Med 35:1369–1375
8. Pittet JF, Mackersie RC, Martin TR, Matthay MA (1997) Biological markers of acute lung injury: prognostic and pathogenetic significance. Am J Respir Crit Care Med 155:1187–1205
9. Reynolds HY (2005) Lung inflammation and fibrosis: an alveolar macrophage-centered perspective from the 1970 s to 1980 s. Am J Resp Crit Care Med 171:98–102
10. Lee WL, Downey GP (2001) Neutrophil activation and acute lung injury. Curr Opin Crit Care 7:1–7
11. Dos Santos CC (2008) Advances in mechanisms of repair and remodelling in acute lung injury. Intensive Care Med 34:619–630
12. Pawlik MT, Schubert T, Hopf S, Lubnow M, Gruber M, Selig C, Taeger K, Ittner KP (2009) The effects of fenoterol inhalation after acid aspiration-induced lung injury. Anesth Analg 109:143–150

13. Trabold B, Pawlik M, Nietsch R, Bitzinger DI, Gruber M, Ittner KP, Lubnow M (2009) Bosentan reduces oxidative burst in acid aspiration-induced lung injury in rats. Injury 40:946–949

14. Jian MY, Koizumi T, Tsushima K, Yokoyama T, Kubo K, Baba A (2010) Exogenous surfactant instillation attenuates inflammatory response to acid-induced lung injury in rat. Pulm Pharmacol Ther 23:43–47

15. Boost KA, Hoegl S, Hofstetter C, Flondor M, Stegewerth K, Platacis I, Pfeilschifter J, Muhl H, Zwissler B (2007) Targeting caspase-1 by inhalation-therapy: effects of Ac-YVAD-CHO on IL-1 beta, IL-18 and downstream proinflammatory parameters as detected in rat endotoxaemia. Intensive Care Med 33:963–971

16. Bueltmann M, Kong X, Mertens M, Yin N, Yin J, Liu Z, Koster A, Kuppe H, Kuebler WM (2009) Inhaled milrinone attenuates experimental acute lung injury. Intensive Care Med 35:171–178

17. Chen DL, Bedient TJ, Kozlowski J, Rosenbluth DB, Isakow W, Ferkol TW, Thomas B, Mintun MA, Schuster DP, Walter MJ (2009) [18F]fluorodeoxyglucose positron emission tomography for lung anti-inflammatory response evaluation. Am J Resp Crit Care Med 180:533–539

18. Bellani G, Messa C, Guerra L, Spagnolli E, Foti G, Patroniti N, Fumagalli R, Musch G, Fazio F, Pesenti A (2009) Lungs of patients with acute respiratory distress syndrome show diffuse inflammation in normally aerated regions: A [18F]-fluoro-2-deoxy-D-glucose PET/CT study. Crit Care Med 37:2216–2222

19. Rodrigues RS, Miller PR, Bozza FA, Marchiori E, Zimmerman GA, Hoffman JM, Morton KA (2008) FDG-PET in patients at risk for acute respiratory distress syndrome: a preliminary report. Intensive Care Med 34:2273–2278

20. Bellani G, Guerra L, Musch G, Zanella A, Patroniti N, Mauri T, Messa C, Pesenti A (2011) Lung regional metabolic activity and gas volume changes induced by tidal ventilation in patients with acute lung injury. Am J Respir Crit Care Med 183:1193–1199

21. Musch G, Venegas JG, Bellani G, Winkler T, Schroeder T, Petersen B, Harris RS, Melo MF (2007) Regional gas exchange and cellular metabolic activity in ventilator-induced lung injury. Anesthesiology 106:723–735

22. Costa EL, Musch G, Winkler T, Schroeder T, Harris RS, Jones HA, Venegas JG, VidalMelo MF (2010) Mild endotoxemia during mechanical ventilation produces spatially heterogeneous pulmonary neutrophilic inflammation in sheep. Anesthesiology 112:658–669

23. Chen DL, Schuster DP (2004) Positron emission tomography with [18F]fluorodeoxyglucose to evaluate neutrophil kinetics during acute lung injury. Am J Physiol Lung Cell Mol Physiol 286:L834–L840

24. Zhou Z, Kozlowksi J, Goodrich AL, Markman N, Chen DL, Schuster DP (2005) Molecular imaging of lung glucose uptake after endotoxin in mice. Am J Physiol Lung Cell Mol Physiol 289:L760–L768

25. Zhou Z, Kozlowski J, Schuster DP (2005) Physiologic, biochemical, and imaging characterization of acute lung injury in mice. Am J Respir Crit Care Med 172:344–351

26. Jones HA, Schofield J, Krausz T, Boobis A, Haslett C (1998) Pulmonary fibrosis correlates with duration of tissue neutrophil activation. Am J Respir Crit Care Med 158:620–628

27. Jones HA, Clark RJ, Rhodes CG, Schofield JB, Krausz T, Haslett C (1994) In vivo measurement of neutrophil activity in experimental lung inflammation. Am J Respir Crit Care Med 149:1635–1639

28. Chen DL, Rosenbluth DB, Mintun MA, Schuster DP (2006) FDG-PET imaging of pulmonary inflammation in healthy volunteers after airway instillation of endotoxin. J Appl Physiol 100:1602–1609

29. Jones HA, Sriskandan S, Peters A, Pride N, Krausz T (1997) Dissociation of neutrophil emigration and metabolic activity in lobar pneumonia and bronchiectasis. Eur Respir J 10:795–803

30. Oehler R, Weingertmann G, Manhart N, Salzer U, Meissner M, Schlegel W, Spittler A, Bergmann M, Kandioler D, Oismüller C, Struse HM, Roth E (2000) Polytrauma induces increased expression of pyruvate kinase in neutrophils. Blood 95:1086–1092

31. Tager AM, Kradin RL, LaCamera P, Bercury SD, Campanella GSV, Leary CP, Polosukhin V, Zhao LH, Sakamoto H, Blackwell TS, Luster AD (2004) Inhibition of pulmonary fibrosis by the chemokine IP-10/CXCL10. Am J Respir Cell Mol Biol 31:395–404

32. Li G, Malinchoc M, Cartin-Ceba R, Venkata CV, Kor DJ, Peters SG, Hubmayr RD, Gajic O (2011) Eight-year trend of acute respiratory distress syndrome: a population-based study in Olmsted County, Minnesota. Am J Respir Crit Care Med 183:59–66

33. Reutershan J, Basit A, Galkina EV, Ley K (2005) Sequential recruitment of neutrophils into lung and bronchoalveolar lavage fluid in LPS-induced acute lung injury. Am J Physiol Lung Cell Mol Physiol 298:L807–L815

34. Reiss M, Roos D (1978) Differences in oxygen metabolism of phagocytosing monocytes and neutrophils. J Clin Invest 61:480–488

35. Nagagawa A, Nathan CF, Cohn ZA (1981) Hydrogen peroxide metabolism in human monocytes during differentiation in vitro. J Clin Invest 68:1243–1252

36. Deichen JT, Prante O, Gack M, Schmiedehausen K, Kuwert T (2003) Uptake of [18F]fluorodeoxyglucose in human monocyte-macrophages in vitro. Eur J Nucl Med Mol Imaging 30:267–273

37. Gamelli RL, Liu H, He LK, Hofmann CA (1996) Augmentations of glucose uptake and glucose transporter-1 in macrophages following thermal injury and sepsis in mice. J Leukoc Biol 59:639–647

38. Kubota R, Yamada S, Kubota K, Ishiwata K, Tamahashi N, Ido T (1992) Intratumoral distribution of fluorine-18-fluorodeoxyglucose in vivo: high accumulation in macrophages and granulation tissues studied by microautoradiography. J Nucl Med 33:1972–1980

39. Pawlik MT, Lubnow M, Gruber M, Taeger K, Riegger G, Pfeifer M, Ittner K (2009) Hydrochloric acid aspiration increases right ventricular systolic pressure in rats. Eur J Anaesthesiol 26:285–292

40. Kubota R, Yamada S, Kubota K, Ishiwata K, Ido T (1993) Micro-autoradiographic method to study [18F]FDG uptake in mouse tissue. Nucl Med Biol 20:183–188

41. Canat X, Guillaumont A, Bouaboula M, Poinot-Chazel C, Derocq JM, Carayon P, LeFur G, Casellas P (1993) Peripheral benzodiazepine receptor modulation with phagocyte differentiation. Biochem Pharmacol 46:551–554

42. Branley HM, du Bois RM, Wells AU, Jones HA (2007) Peripheral-type benzodiazepine receptors in bronchoalveolar lavage cells of patients with interstitial lung disease. Nucl Med Biol 34:553–558